Probabilistic Slope Stability Analysis by Finite Elements

D. V. Griffiths, F.ASCE,[1] and Gordon A. Fenton, M.ASCE[2]

Abstract: In this paper we investigate the probability of failure of a cohesive slope using both simple and more advanced probabilistic analysis tools. The influence of local averaging on the probability of failure of a test problem is thoroughly investigated. In the simple approach, classical slope stability analysis techniques are used, and the shear strength is treated as a single random variable. The advanced method, called the random finite-element method (RFEM), uses elastoplasticity combined with random field theory. The RFEM method is shown to offer many advantages over traditional probabilistic slope stability techniques, because it enables slope failure to develop naturally by ''seeking out'' the most critical mechanism. Of particular importance in this work is the conclusion that simplified probabilistic analysis, in which spatial variability is ignored by assuming perfect correlation, can lead to unconservative estimates of the probability of failure. This contradicts the findings of other investigators who used classical slope stability analysis tools.

DOI: 10.1061/(ASCE)1090-0241(2004)130:5(507)

CE Database subject headings: Slope stability; Finite elements; Probabilitic methods; Failures.

Introduction

Slope stability analysis is a branch of geotechnical engineering that is highly amenable to probabilistic treatment, and it has received considerable attention in the literature. The earliest papers appeared in the 1970s (e.g., Matsuo and Kuroda 1974; Alonso 1976; Tang et al. 1976; Vanmarcke 1977) and have continued steadily (e.g., D'Andrea and Sangrey 1982; Chowdhury and Tang 1987; Li and Lumb 1987; Mostyn and Li 1992; Christian et al. 1994; Lacasse 1994; Christian 1996; Lacasse and Nadim 1996; Wolff 1996; Duncan 2000; Hassan and Wolff 2000; Whitman 2000). Most recently, El-Ramly et al. (2002) produced a useful review of the literature on this topic, and also noted that the geotechnical profession was slow to adopt probabilistic approaches to geotechnical design, especially for traditional problems such as slopes and foundations.

Two main observations can be made in relation to the existing body of work on this subject. First, the vast majority of probabilistic slope stability analyses, while using novel and sometimes quite sophisticated probabilistic methodologies, continue to use classical slope stability analysis techniques (e.g., Bishop 1955) that have changed little in decades, and were never intended for use with highly variable soil shear strength distributions. An obvious deficiency of traditional slope stability approaches is that the shape of the failure surface (e.g., circular) is often fixed by the method, thus the failure mechanism is not allowed to ''seek out'' the most critical path through the soil. Second, while the importance of spatial correlation (or autocorrelation) and local averaging of statistical geotechnical properties has long been recognized by some investigators (e.g., Mostyn and Soo 1992), it is still regularly omitted from many probabilistic slope stability analyses. In recent years, the present authors have been pursuing a more rigorous method of probabilistic geotechnical analysis (e.g., Fenton and Griffiths 1993; Paice 1997; Griffiths and Fenton 2000), in which nonlinear finite-element methods are combined with random field generation techniques. This method, called here the ''random finite-element method'' (RFEM), fully accounts for spatial correlation and averaging, and is also a powerful slope stability analysis tool that does not require a priori assumptions related to the shape or location of the failure mechanism.

In order to demonstrate the benefits of this method and to put it into context, in this paper we investigate the probabilistic stability characteristics of a cohesive slope using both the simple and more advanced methods. Initially, the slope is investigated using simple probabilistic concepts and classical slope stability techniques, followed by an investigation on the role of spatial correlation and local averaging. Finally, results are presented from a full-blown RFEM approach. Where possible throughout this paper, the probability of failure (p_f) is compared with the traditional factor of safety (FS) that would be obtained from charts or classical limit equilibrium methods.

The slope under consideration, known as the ''test problem'' is shown in Fig. 1, and consists of undrained clay, with shear strength parameters $\phi_u = 0$ and c_u. In this study, the slope inclination and dimensions, given by β, H, and D, and the saturated unit weight of the soil, γ_{sat}, are held constant, while the undrained shear strength c_u is assumed to be a random variable. In the interest of generality, the undrained shear strength will be expressed in dimensionless form C, where $C = c_u/(\gamma_{sat} H)$.

Probabilistic Description of Shear Strength

In this study, shear strength C is assumed to be characterized statistically by a log–normal distribution defined by a mean, μ_C, and a standard deviation σ_C.

The probability density function of a log–normal distribution is given by

[1]Professor, Geomechanics Research Center, Colorado School of Mines, Golden, CO 80401.

[2]Professor, Dept. of Engineering Mathematics, Dalhousie Univ., Halifax NS, Canada B3H 4R2.

Note. Discussion open until October 1, 2004. Separate discussions must be submitted for individual papers. To extend the closing date by one month, a written request must be filed with the ASCE Managing Editor. The manuscript for this paper was submitted for review and possible publication on December 31, 2002; approved on June 9, 2003. This paper is part of the ***Journal of Geotechnical and Geoenvironmental Engineering***, Vol. 130, No. 5, May 1, 2004. ©ASCE, ISSN 1090-0241/2004/5-507–518/$18.00.

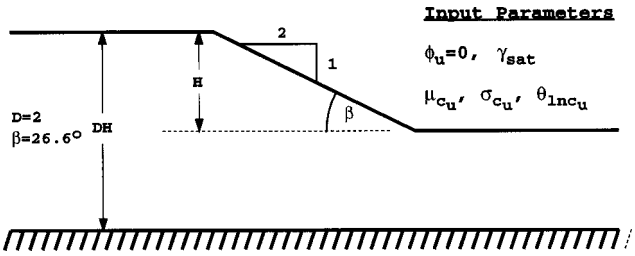

Fig. 1. Cohesive slope test problem

$$f(C)=\frac{1}{C\sigma_{\ln C}\sqrt{2\pi}}\exp\left[-\frac{1}{2}\left(\frac{\ln C-\mu_{\ln C}}{\sigma_{\ln C}}\right)^2\right] \quad (1)$$

shown in Fig. 2 for a typical case with $\mu_C=100\,\text{kN/m}^2$ and $\sigma_C=50\,\text{kN/m}^2$. The function encloses an area of unity, thus the probability of the strength dropping below a given value is easily found from standard tables. The mean and standard deviation can conveniently be expressed in terms of the dimensionless coefficient of variation, defined as

$$V_C=\frac{\sigma_C}{\mu_C} \quad (2)$$

Other useful relationships that relate to the log–normal function include the standard deviation and mean of the underlying normal distribution as follows:

$$\sigma_{\ln C}=\sqrt{\ln\{1+V_C^2\}} \quad (3)$$

$$\mu_{\ln C}=\ln\mu_C-\tfrac{1}{2}\sigma_{\ln C}^2 \quad (4)$$

Rearrangement of Eqs. (3) and (4) gives the inverse relationships

$$\mu_C=\exp(\mu_{\ln C}+\tfrac{1}{2}\sigma_{\ln C}^2) \quad (5)$$

$$\sigma_C=\mu_C\sqrt{\exp(\sigma_{\ln C}^2)-1} \quad (6)$$

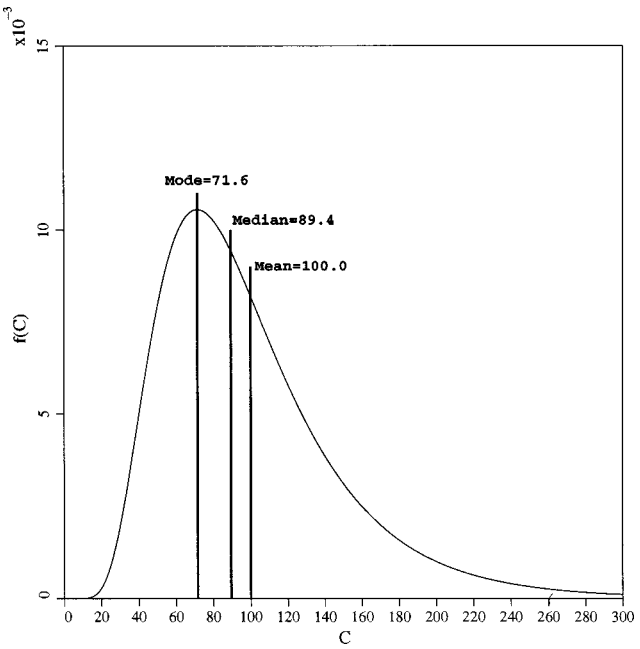

Fig. 2. Typical log–normal distribution with mean of 100 and standard deviation of 50 ($V_C=0.5$)

Table 1. Factors of Safety Assuming Homogeneous Soil

C	Factor of safety
0.15	0.88
0.17	1.00
0.20	1.18
0.25	1.47
0.30	1.77

Finally the median and mode of a log–normal distribution are given by

$$\text{median}_C=\exp(\mu_{\ln C}) \quad (7)$$

$$\text{mode}_C=\exp(\mu_{\ln C}-\sigma_{\ln C}^2) \quad (8)$$

A third parameter, the spatial correlation length $\theta_{\ln C}$ will also be considered in this study. Since the actual undrained shear strength field is log normally distributed, its logarithm yields an "underlying" normal distributed (or Gaussian) field. The spatial correlation length is measured with respect to this underlying field, that is, with respect to $\ln C$. The spatial correlation length ($\theta_{\ln C}$) describes the distance over which the spatially random values will tend to be significantly correlated in the underlying Gaussian field. Thus, a large value of $\theta_{\ln C}$ will imply a smoothly varying field, while a small value will imply a ragged field. The spatial correlation length can be estimated from a set of shear strength data taken over some spatial region simply by performing statistical analyses on the log data. In practice, however, $\theta_{\ln C}$ is not much different in magnitude from the correlation length in real space and, for most purposes, θ_C and $\theta_{\ln C}$ are interchangeable given their inherent uncertainty in the first place. In the current study, the spatial correlation length has been nondimensionalized by dividing it by the height of embankment H and will be expressed in the form,

$$\Theta_C=\theta_{\ln C}/H \quad (9)$$

It has been suggested (see, e.g., Lee et al. 1983; Kulhawy et al. 1991) that typical V_C values for undrained shear strength lie in the range of 0.1–0.5. The spatial correlation length, however, is less well documented and may well exhibit anisotropy, especially in the horizontal direction. While the advanced analysis tools used later in this study have the capability of modeling an anisotropic spatial correlation field, the spatial correlation, when considered, will be assumed to be isotropic.

Preliminary Deterministic Study

To put the probabilistic analyses into context, an initial deterministic study has been performed assuming a homogeneous soil. For the simple slope shown in Fig. 1, the factor of safety can readily be obtained from Taylor's (1937) charts or simple limit equilibrium methods to give the data in Table 1.

These results, plotted in Fig. 3, indicate the linear relationship between C and FS. Fig. 3 also shows that the test slope becomes unstable when the shear strength parameter falls below $C=0.17$.

Single Random Variable Approach

The first probabilistic analysis presented here investigates the influence of giving the shear strength C a log–normal probability

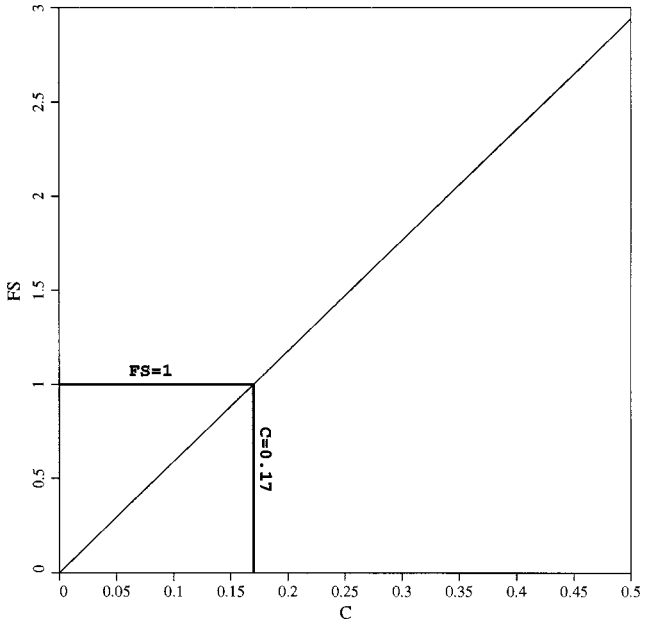

Fig. 3. Linear relationship between factor of safety and C for a cohesive slope with slope angle of $\beta=26.57°$ and depth ratio of $D=2$

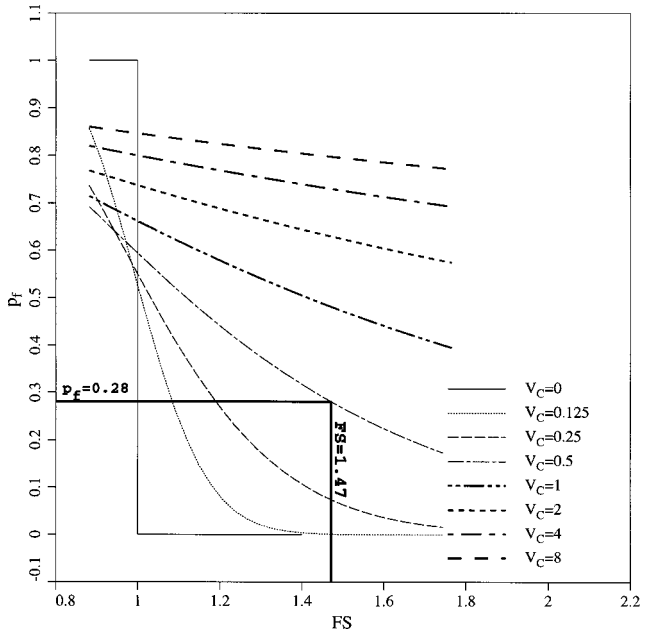

Fig. 4. Probability of failure versus factor of safety (based on the mean) in single random variable approach; the mean is fixed at $\mu_C=0.25$

density function similar to that shown in Fig. 2, based on a mean μ_C and a standard deviation σ_C. The slope is assumed to have the same value of C everywhere, however the value of C is selected randomly from the log–normal distribution. Anticipating the random field analyses that will be described later in this paper, this ''single random variable (SRV) approach'' implies a spatial correlation length of $\Theta_C=\infty$, so no local averaging is applicable.

The probability of failure (p_f) in this case, is simply equal to the probability that the shear strength parameter C will be less than 0.17. Quantitatively, this is equal to the area of the probability density function that corresponds to $C\leqslant 0.17$.

For example, if $\mu_C=0.25$ and $\sigma_C=0.125$ ($V_C=0.5$), Eqs. (3) and (4) give the mean and standard deviation of the underlying *normal* distribution of the strength parameter as $\mu_{\ln C}=-1.498$ and $\sigma_{\ln C}=0.472$.

The probability of failure is therefore given by

$$p_f=p[C<0.17]=\Phi\left(\frac{\ln 0.17-\mu_{\ln C}}{\sigma_{\ln C}}\right)=0.281 \qquad (10)$$

where Φ=cumulative standard normal distribution function.

This approach has been repeated for a range of μ_C and V_C values, for the slope under consideration, and it leads to Fig. 4 which gives a direct relationship between the factor of safety and the probability of failure. It should be emphasized that the factor of safety in this plot is based on the value that would have been obtained if the slope had consisted of homogeneous soil with a shear strength equal to the mean value μ_C in Fig. 3. From Fig. 4, the probability of failure (p_f) clearly increases as the factor of safety decreases, however it is also shown that, for FS$>$1, the probability of failure increases as V_C increases. The exception to this trend occurs when FS$<$1. As shown in Fig. 4, the probability of failure in such cases is understandably high, however the role of V_C has the opposite effect, with lower values of V_C tending to give the highest values of the probability of failure. This is explained by the ''bunching up'' of the shear strength distribution at low V_C rapidly excluding area to the right of the critical value of $C=0.17$. Fig. 5 shows that the median$_C$ is key to understanding how the probability of failure changes in this analysis. When median$_C<0.17$, increasing V_C causes p_f to fall, whereas when median$_C>0.17$, increasing V_C causes p_f to rise.

While the single random variable approach described in this section leads to simple calculations and useful qualitative comparisons between the probability of failure and the factor of safety, the quantitative merit of the approach is more questionable. An important observation highlighted in Fig. 4 is that soil with a mean strength of $\mu_C=0.25$ (implying FS=1.47) would give a probability of failure as high as $p_f=0.28$ for soil with $V_C=0.5$. Practical experience indicates that slopes with a factor of safety as high as FS=1.47 rarely fail.

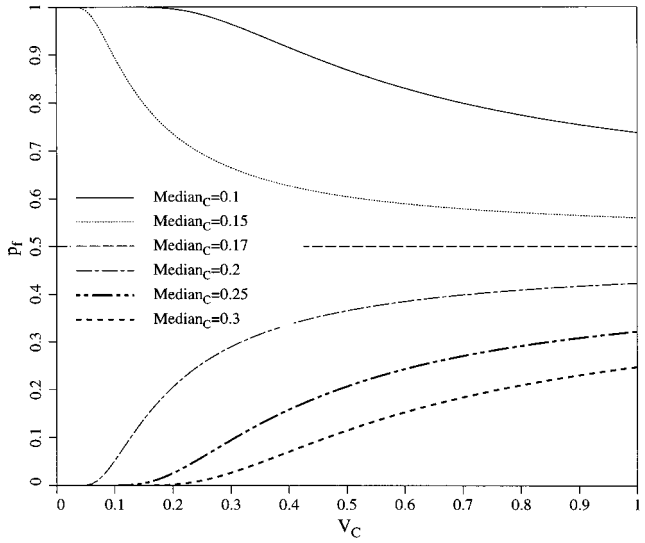

Fig. 5. p_f versus V_C for different median$_C$ values

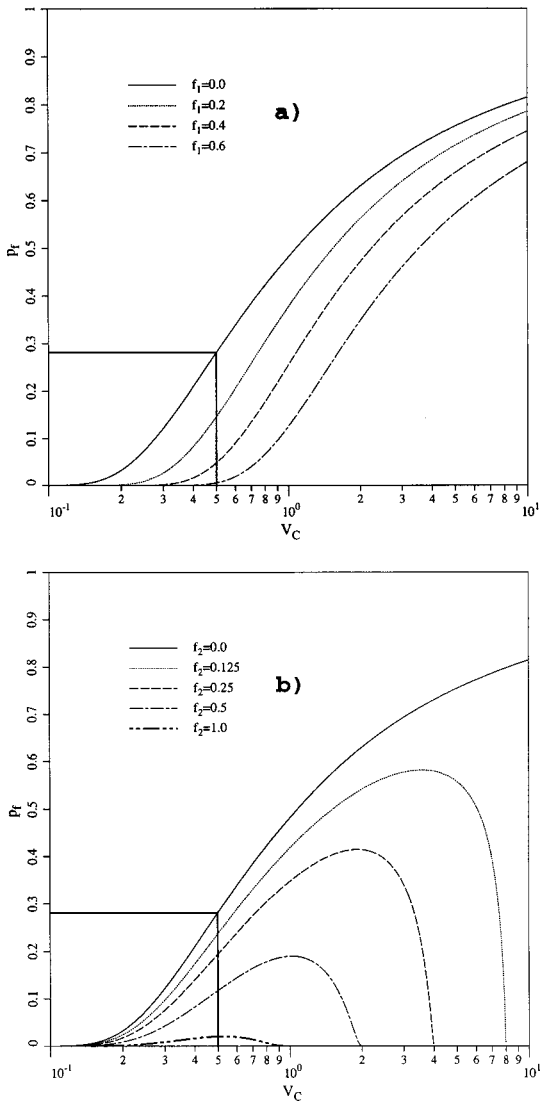

Fig. 6. Influence of different mean strength factoring strategies on probability of failure versus factor of safety relationship: (a) linear factoring and (b) standard deviation factoring; all curves assume factor of safety =1.47 (based on $C_{\text{des}}=0.25$)

An implication of this result is that either the perfectly correlated single random variable approach is entirely pessimistic in the prediction of the probability of failure, and/or it is unconservative to use the mean strength of variable soil to estimate the factor of safety. Presented with a range of shear strengths at a given site, a geotechnical engineer would likely select a ''pessimistic'' or ''lowest plausible'' value for design, C_{des}, that would be lower than the mean. Assuming for the time being that the single random variable approach is reasonable, Fig. 6 shows the influence on the probability of failure of two strategies for factoring the mean strength μ_C prior to calculating the factor of safety for the test problem. In Fig. 6(a), linear reduction in the mean strength has been proposed using a factor, f_1, where

$$C_{\text{des}}=\mu_C(1-f_1) \tag{11}$$

and in Fig. 6(b), the mean strength has been reduced by a factor, f_2, of the standard deviation, where

$$C_{\text{des}}=\mu_C-f_2\sigma_C \tag{12}$$

All the results shown in Fig. 6 assume that after factorization, $C_{\text{des}}=0.25$, implying a factor of safety of FS=1.47. The probability of failure of $p_f=0.28$ with no factorization, $f_1=f_2=0$, has also been highlighted for the case of $V_C=0.5$. In both cases, an increase in the strength reduction factor reduces the probability of failure, which is to be expected, however, the nature of the two sets of reduction curves is quite different, especially for higher values of V_C. From the linear mean strength reduction [Eq. (11)], $f_1=0.6$ would result in a probability of failure of about 0.6%. By comparison, a mean strength reduction of one standard deviation given by $f_2=1$ [Eq. (12)] would result in a probability of failure of about 2%. Fig. 6(a) shows a gradual reduction of the probability of failure for all values of f_1 and V_C, however quite different behavior is shown in Fig. 6(b), where standard deviation factoring results in very rapid reduction of the probability of failure, especially for higher values of $V_C>2$. This curious result is easily explained by the functional relationship between p_f and V_C, where the design strength can be written as

$$C_{\text{des}}=0.25=\mu_C-f_2\sigma_C=\mu_C(1-f_2V_C) \tag{13}$$

hence as $V_C\rightarrow 1/f_2$, $\mu_C\rightarrow\infty$. With the mean strength so much greater than the critical value of 0.17, the probability of failure falls very rapidly towards 0.

Spatial Correlation

Implicit in the single random variable approach described above is that the spatial correlation length is infinite. In other words, only homogeneous slopes are considered, in which the property assigned to the slope is taken at random from a log–normal distribution. A more realistic model would properly take into account smaller spatial correlation lengths in which the soil strength is allowed to vary spatially within the slope. The parameter that controls this is the spatial correlation length $\theta_{\ln C}$, discussed earlier. In this work, an exponentially decaying (Markovian) correlation function of the following form is used:

$$\rho=e^{-(2\tau/\theta_{\ln C})} \tag{14}$$

where ρ=familiar correlation coefficient; and τ=absolute distance between two points in a random field. A plot of this function is given in Fig. 7 and it indicates, for example, that the strength at two points separated by $\theta_{\ln C}(\tau/\theta_{\ln C}=1)$ will have an expected correlation of $\rho=0.135$. This correlation function is merely a way of representing the field observation that soil samples taken close together are more likely to have similar properties than samples taken far apart. There is also the issue of anisotropic spatial correlation, in that soil is likely to have longer spatial correlation lengths in the horizontal direction than in the vertical, due to depositional history. While the tools described in this paper can take anisotropy into account, this refinement is left for future studies.

Random Finite-Element Method

A powerful general method of accounting for spatially random shear strength parameters and spatial correlation is the random finite-element method which combines elastoplastic finite-element analysis with random field theory generated using the local average subdivision method (Fenton and Vanmarcke 1990). The methodology has been described in detail in other publications (e.g., Griffiths and Fenton 2001), so only a brief description will be given here.

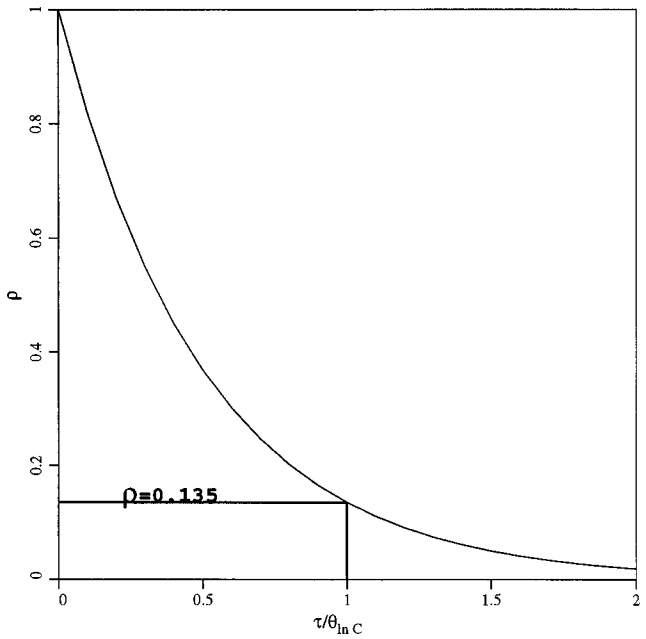

Fig. 7. Markov correlation function

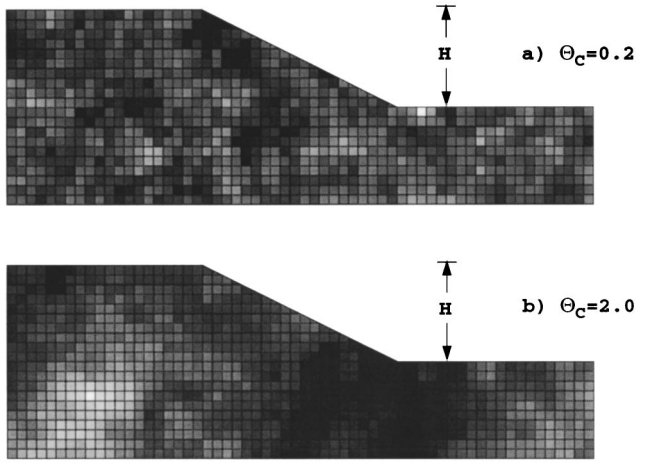

Fig. 9. Influence of scale of fluctuation in random finite-element method analysis

A typical finite-element mesh for the test problem considered in this paper is shown in Fig. 8. The majority of the elements are square, however the elements adjacent to the slope have degenerated into triangles.

The code developed by the writers enables a random field of shear strength values to be generated and mapped onto the finite-element mesh taking into full account the element size in the local averaging process. In a random field, the value assigned to each cell (or finite element in this case) is itself a random variable, thus the mesh in Fig. 8, which has 910 finite elements, contains 910 random variables. The random variables can be correlated to one another by controlling the spatial correlation length $\theta_{\ln C}$ described earlier, hence the single random variable approach discussed in ''Spatial Correlation'' where the spatial correlation length is implicitly set to infinity can now be viewed as a special case of a much more powerful analytical tool. Figs. 9(a and b) show typical meshes that correspond to different spatial correlation lengths. Fig. 9(a) shows a relatively low spatial correlation length of $\Theta_C=0.2$ and Fig. 9(b) shows a relatively high spatial correlation length of $\Theta_C=2$. Dark and light regions depict ''weak'' and ''strong'' soil, respectively. It should be emphasized that both these shear strength distributions come from the same log–normal distribution, and it is only the spatial correlation length that is different.

In brief, the analyses involve the application of gravity loading and the monitoring of stress at all Gauss points. The slope stability analyses use an elastic-perfectly plastic stress–strain law with a Tresca failure criterion which is appropriate for ''undrained clays.'' If the Tresca criterion is violated, the program attempts to redistribute excess stress to neighboring elements that still have reserves of strength. This is an iterative process which continues until the Tresca criterion and global equilibrium are satisfied at all points within the mesh under quite strict tolerances.

Plastic stress redistribution is accomplished using a viscoplastic algorithm with 8-node quadrilateral elements and reduced integration in both the stiffness and stress redistribution parts of the algorithm. The theoretical basis of the method is described more fully in Chap. 6 of the text by Smith and Griffiths (1998), and for a detailed discussion of the method applied to slope stability analysis, the reader is referred to work by Griffiths and Lane (1999).

For a given set of input shear strength parameters (mean, standard deviation, and spatial correlation length), Monte Carlo simulations are performed. This means that the slope stability analysis is repeated many times until the statistics of the output quantities of interest become stable. Each ''realization'' of the Monte Carlo process differs in the locations at which the strong and weak zones are situated. For example, in one realization, weak soil may be situated in locations where a critical failure mechanism develops causing the slope to fail, whereas in another, strong soil in those locations means that the slope remains stable.

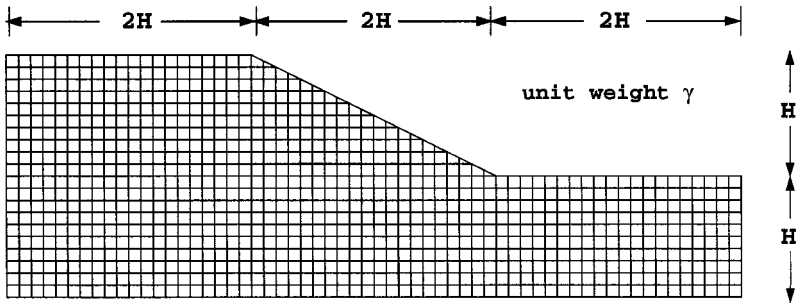

Fig. 8. Mesh used for random finite-element method slope stability analyses

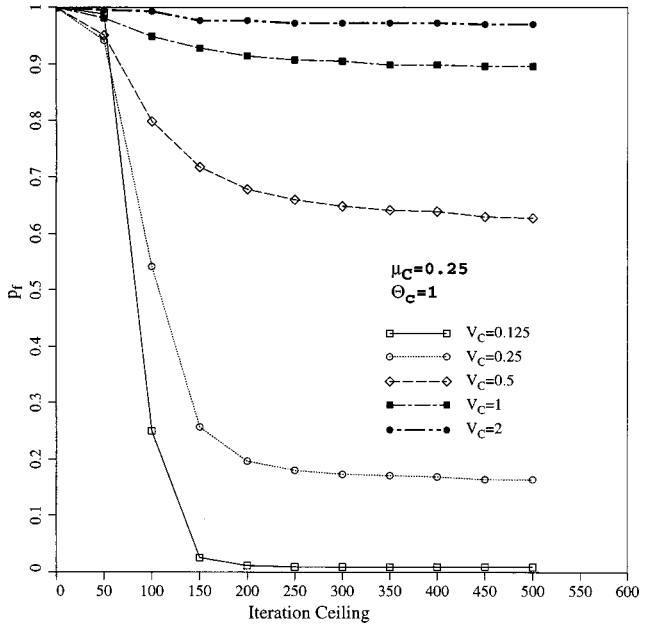

Fig. 10. Influence of plastic iteration ceiling on computed probability of failure

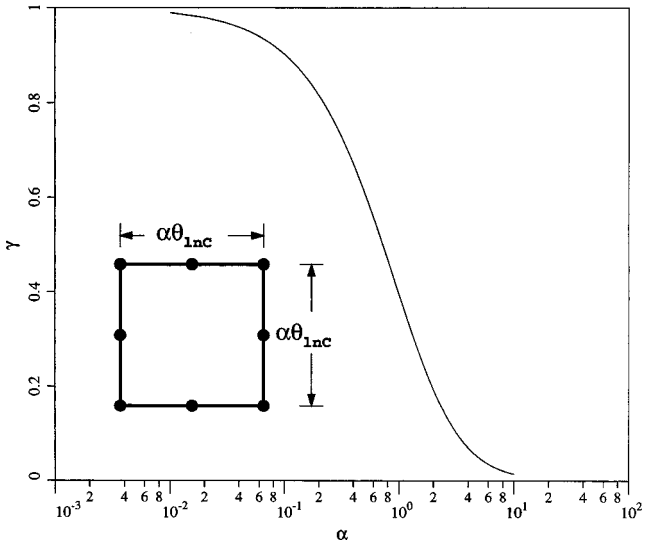

Fig. 11. Variance reduction function over a square element of side length $\alpha\theta_{\ln C}$ with a Markov correlation function

In this study, it was determined that 1,000 realizations of the Monte Carlo process for each parametric group was sufficient to give reliable reproducible estimates of the probability of failure, which was simply defined as the proportion of 1,000 Monte Carlo slope stability analyses that failed.

In this study, ''failure'' is said to have occurred if, for any given realization, the algorithm was unable to converge within 500 iterations. While the choice of 500 as the iteration ceiling is subjective, Fig. 10 confirms, for the case of $\mu_C=0.25$ and $\Theta_C=1$, that the probability of failure defined this way is stable for iteration ceilings greater than about 200.

Local Averaging

The input parameters that relate to the mean, standard deviation, and spatial correlation length of the undrained strength are assumed to be defined at the point level. While statistics at this resolution are obviously impossible to measure in practice, they represent a fundamental baseline of the inherent soil variability which can be corrected through local averaging to take in to account the sample size.

Within the context of the RFEM approach, each element is assigned a constant property at each realization of the Monte Carlo process. The ''sample'' is represented by the size of each finite element used to discretize the slope. If the point distribution is normal, local averaging results in reduced variance but the mean is unaffected. In a log–normal distribution, however, both the mean and the standard deviation are reduced by local averaging. This is because, from Eqs. (5) and (6), the mean of a log–normal relationship depends on both the mean and the variance of the underlying normal relationship. Thus the cruder the discretization of the slope stability problem and larger the elements, the greater the influence of local averaging in the form of reduced mean and standard deviation. These adjustments to the point statistics are fully accounted for in the RFEM, and are implemented before the elastoplastic finite-element slope stability analysis takes place.

Variance Reduction over a Square Finite Element

Here, an algorithm used to compute the locally averaged statistics applied to the mesh is described.

A log–normal distribution of random variable C, with point statistics given by mean μ_C, standard deviation σ_C, and spatial correlation length $\theta_{\ln C}$ is mapped onto a mesh of square finite elements. Each element is assigned a single value of the undrained strength parameter.

The locally averaged statistics over the elements will be referred to here as the ''area'' statistics by subscript A. Thus, with reference to the underlying normal distribution of $\ln C$, the mean, which is unaffected by local averaging, is given by $\mu_{\ln C_A}$, and the standard deviation, which is affected by local averaging, is given by $\sigma_{\ln C_A}$.

The variance reduction factor due to local averaging γ, is defined as

$$\gamma=\left(\frac{\sigma_{\ln C_A}}{\sigma_{\ln C}}\right)^2 \tag{15}$$

and is a function of the element size and the correlation function from Eq. (14), repeated here in the form,

$$\rho=\exp\left(-\frac{2}{\theta_{\ln C}}\sqrt{\tau_x^2+\tau_y^2}\right) \tag{16}$$

where τ_x=difference between the x coordinates of any two points in the random field; and τ_y=difference between the y coordinates.

For a square finite element of side length $\alpha\theta_{\ln C}$, shown in Fig. 11, it can be shown (Vanmarcke 1984) that, for an isotropic spatial correlation field, the variance reduction factor is given by

$$\gamma=\frac{4}{(\alpha\theta_{\ln C})^4}\int_0^{\alpha\theta_{\ln C}}\int_0^{\alpha\theta_{\ln C}}\exp\left(-\frac{2}{\theta_{\ln C}}\sqrt{x^2+y^2}\right)(\alpha\theta_{\ln C}-x)$$
$$\times(\alpha\theta_{\ln C}-y)dxdy \tag{17}$$

Numerical integration of this function leads to the variance reduction values given in Table 2 and plotted in Fig. 11.

Fig. 11 indicates that elements that are small relative to the correlation length ($\alpha\to 0$) lead to very little reduction in variance

Table 2. Reduction in Variance over a Square Element

α	γ
0.01	0.9896
0.1	0.9021
1	0.3965
10	0.0138

($\gamma \rightarrow 1$), whereas elements that are large relative to the correlation length can lead to very significant variance reduction ($\gamma \rightarrow 0$).

The statistics of the underlying log field, including local averaging, are therefore given by

$$\sigma_{\ln C_A} = \sigma_{\ln C}\sqrt{\gamma} \tag{18}$$

and

$$\mu_{\ln C_A} = \mu_{\ln C} \tag{19}$$

which leads to the following statistics of the log–normal field, including local averaging, that is actually mapped on the finite-element mesh from Eqs. (5) and (6), thus

$$\mu_{C_A} = \exp(\mu_{\ln C_A} + \tfrac{1}{2}\sigma^2_{\ln C_A}) \tag{20}$$

$$\sigma_{C_A} = \mu_{C_A}\sqrt{\exp(\sigma^2_{\ln C_A}) - 1} \tag{21}$$

It is instructive to consider the range of locally averaged statistics, since this helps to explain the influence of the spatial correlation length $\Theta_C (= \theta_{\ln C}/H)$ on the probability of failure in the RFEM slope analyses that is described in ''Locally Averaged Single Random Variable Approach.''

Expressing the mean and the coefficient of variation of the locally averaged variable as a proportion of the point values of these quantities leads to Figs. 12(a and b), respectively. In both cases, there is virtually no reduction due to local averaging for elements that are small relative to the spatial correlation length ($\alpha \rightarrow 0$). This is to be expected, since the elements are able to model the point field quite accurately. For larger elements relative to the spatial correlation length, however, Fig. 12(a) indicates that the mean of the locally averaged field tends to the median, and Fig. 12(b) indicates that the coefficient of variation of the locally averaged field tends toward zero.

From Eqs. (18)–(21), the expression plotted in Fig. 12(a) for the mean can be written as

$$\frac{\mu_{C_A}}{\mu_C} = \frac{1}{(1+V_C^2)^{(1-\gamma)/2}} \tag{22}$$

which gives the following: When $\gamma \rightarrow 0$, $\mu_{C_A}/\mu_C \rightarrow 1/(1+V_C^2)^{1/2}$, thus $\mu_{C_A} \rightarrow e^{\mu_{\ln C}} = \text{median}_C$. The expression plotted in Fig. 12(b) for the coefficient of variation of the locally averaged variable can be written as

$$\frac{V_{C_A}}{V_C} = \frac{\sqrt{(1+V_C^2)^{\gamma} - 1}}{V_C} \tag{23}$$

which gives the following: when $\gamma \rightarrow 0$, $V_{C_A}/V_C \rightarrow 0$, thus $V_{C_A} \rightarrow 0$.

Further examination of Eqs. (22) and (23) shows that for all values of γ,

$$\text{median}_{C_A} = \text{median}_C \tag{24}$$

hence it can be concluded that

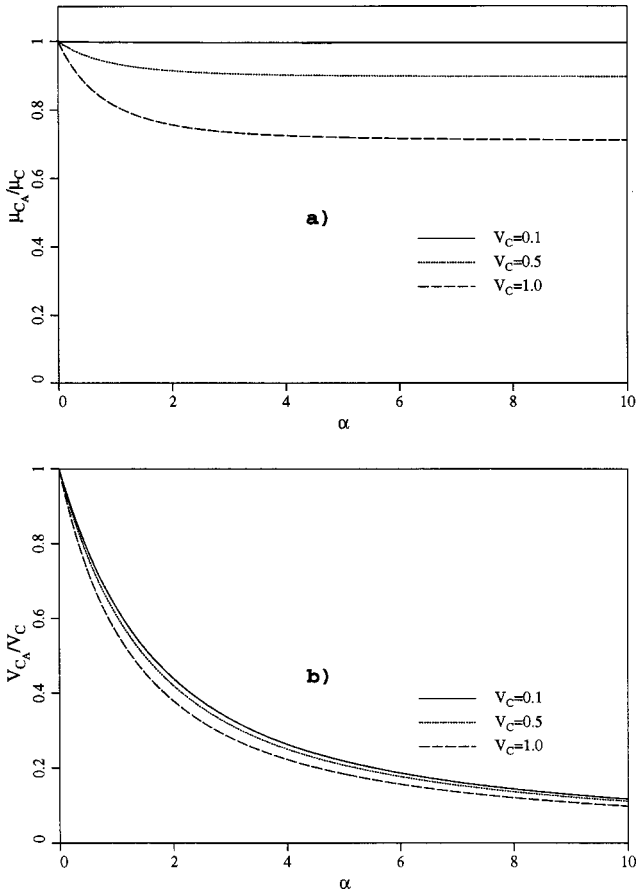

Fig. 12. Influence of element size expressed in the form of a size parameter α on local averaging: influence on the (a) mean and (b) coefficient of variation

1. Local averaging reduces both the mean and the variance of a log–normal point distribution;
2. Local averaging preserves the median of the point distribution; and
3. With significant levels of local averaging, the variance tends to zero and the mean tends to the median.

Locally Averaged Single Random Variable Approach

Here the probability of failure is reworked with the single random variable approach using properties derived from local averaging over an individual finite element, termed ''finite element locally averaged properties'' throughout the rest of this paper. With reference to the mesh shown in Fig. 8, the square elements have a side length of $0.1H$, thus $\Theta_C = 0.1/\alpha$. Fig. 13 shows the probability of failure p_f as a function of Θ_C for a range of input point coefficients of variation, with the point mean fixed at $\mu_C = 0.25$. The probability of failure is defined, as before, by $p(C < 0.17)$, but this time the calculation is based on the finite-element locally averaged properties, μ_{C_A} and σ_{C_A} from Eqs. (20) and (21). Fig. 13 clearly shows two tails to the results, with $p_f \rightarrow 1$ as $\Theta_C \rightarrow 0$ for all $V_C > 1.0783$, and $p_f \rightarrow 0$ as $\Theta_C \rightarrow 0$ for all $V_C < 1.0783$. The horizontal line at $p_f = 0.5$ is given by $V_C = 1.0783$, which is the special value of the coefficient of variation that causes the median_C to equal 0.17. If we recall that, in Table 1, this is the critical value of C that would give FS=1 in the test slope. Higher values of V_C lead to $\text{median}_C < 0.17$ and a tendency for $p_f \rightarrow 1$ as

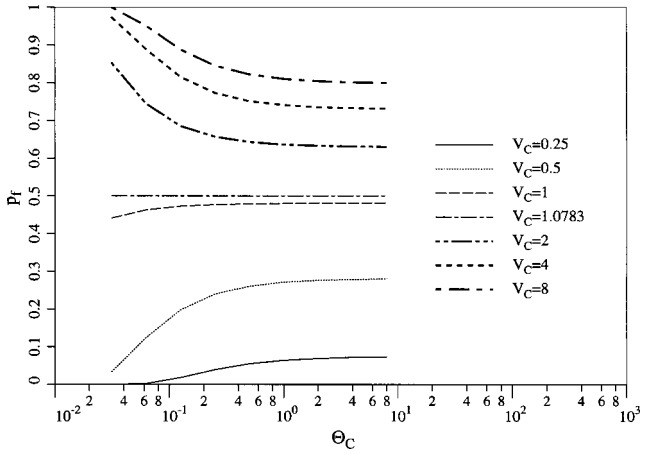

Fig. 13. Probability of failure versus spatial correlation length based on finite-element locally averaged properties; the mean is fixed at $\mu_C=0.25$

$\Theta_C \rightarrow 0$. Conversely, lower values of V_C lead to median$_C > 0.17$ and a tendency for $p_f \rightarrow 0$. Fig. 14 shows the same data plotted the other way round with V_C along the abscissa. Fig. 14 clearly shows the full influence of spatial correlation in the range of $0 \leqslant \Theta_C < \infty$. All the curves cross over at the critical value of $V_C = 1.0783$, and it is of interest to note the step function that corresponds to $\Theta_C = 0$ when p_f changes suddenly from zero to unity.

It should be emphasized that the results presented in this section involved no actual finite-element analysis, and were based solely on a SRV approach using locally averaged properties derived from a typical finite element in a mesh such as that shown in Fig. 8.

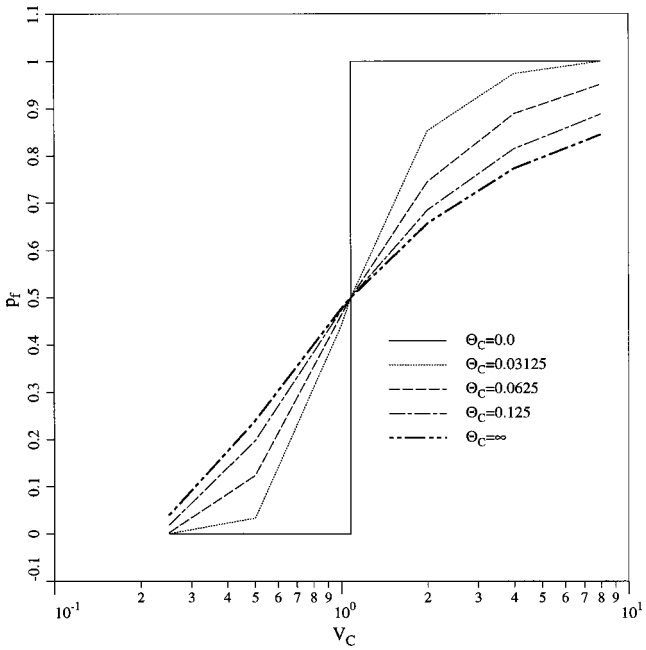

Fig. 14. Probability of failure versus coefficient of variation based on finite-element locally averaged properties; the mean is fixed at $\mu_C=0.25$

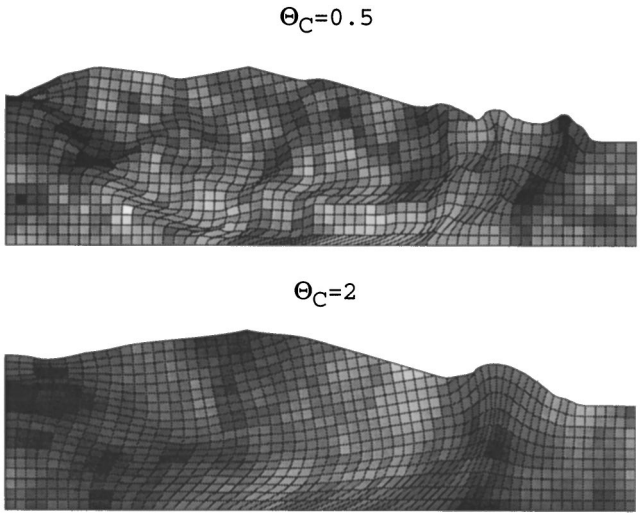

Fig. 15. Typical random field realizations and deformed mesh at slope failure for two different spatial correlation lengths

Results of Random Finite-Element Method Analyses

Now, the results of full nonlinear RFEM analyses with Monte Carlo simulations are described based on a range of parametric variations of μ_C, V_C, and Θ_C.

In the elastoplastic RFEM approach, the failure mechanism is free to "seek out" the weakest path through the soil. Fig. 15 shows two typical random field realizations and the associated failure mechanisms for slopes with $\Theta_C = 0.5$ and 2. The convoluted nature of the failure mechanisms, especially when $\Theta_C = 0.5$, would defy analysis by conventional slope stability analysis tools. While the mechanism is attracted to the weaker zones within the slope, it will inevitably pass through elements assigned many different strength values. This weakest path determination, and the strength averaging that goes with it, occurs quite naturally in the finite-element slope stability method, and represents a very significant improvement over traditional limit equilibrium approaches to probabilistic slope stability analysis. In these traditional methods, if local averaging is included at all, it has to be computed over a failure mechanism that is preset by the particular analysis method (e.g., a circular failure mechanism when using Bishop's method).

In fixing the point mean strength at $\mu_C = 0.25$, Figs. 16 and 17 show the effect of spatial correlation length Θ_C and coefficient of variation V_C on the probability of failure for the test problem. Fig. 16 clearly indicates two branches, with the probability of failure tending toward unity or zero for higher and lower values of V_C, respectively. This behavior is qualitatively similar to that observed in Fig. 13, in which a single random variable approach was used to predict the probability of failure based solely on finite-element locally averaged properties. Fig. 17 shows the same results as Fig. 16, but plotted the other way round with the coefficient of variation along the abscissa. Fig. 17 also shows the theoretically obtained result corresponding to $\Theta_C = \infty$, indicating that a single random variable approach with no local averaging will overestimate the probability of failure (conservative) when the coefficient of variation is relatively small and underestimate the probability of failure (unconservative) when the coefficient of variation is relatively high. Fig. 17 also confirms that the single random variable approach described earlier in the paper, which

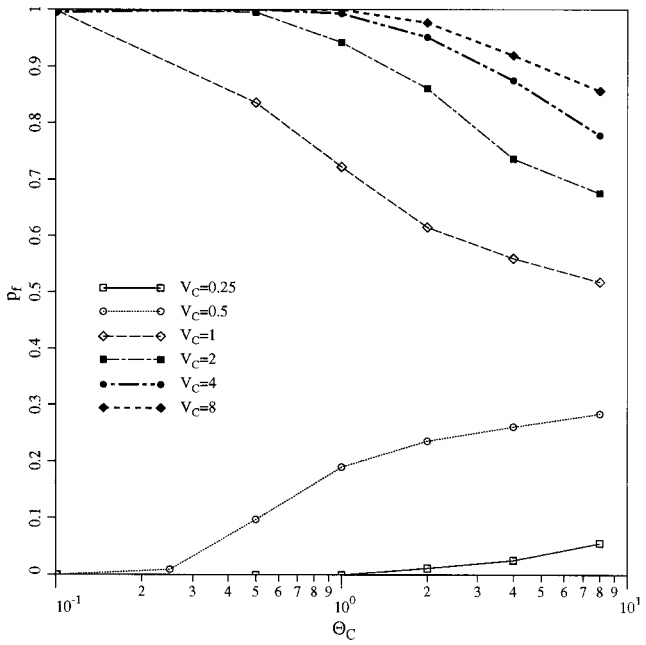

Fig. 16. Probability of failure versus spatial correlation length from random finite-element method; the mean is fixed at $\mu_C=0.25$

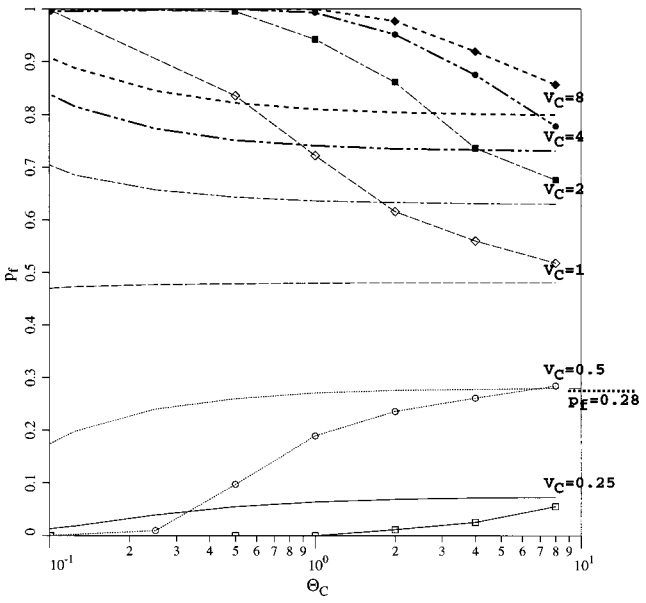

Fig. 18. Comparison of the probability of failure predicted by random finite-element method and by finite-element local averaging only; the curve with points comes from random finite-element method analyses; the mean is fixed at $\mu_C=0.25$

gave $p_f=0.28$ corresponding to $\mu_C=0.25$ and $V_C=0.5$ with no local averaging, is indeed pessimistic. The RFEM results show that the inclusion of spatial correlation and local averaging in this case will always lead to a smaller probability of failure.

Comparison of Figs. 13 and 14 with Figs. 16 and 17 highlights the influence of the finite-element approach to slope stability, where the failure mechanism is free to locate itself optimally within the mesh. From Figs. 14 and 17, it is clear that the ''weakest path'' concept made possible by the RFEM approach has resulted in the crossover point falling to lower values of both V_C and p_f. With only finite-element local averaging, the crossover occurred at $V_C=1.0783$, whereas by the RFEM it occurred at $V_C\approx 0.65$. In terms of the probability of failure with only finite-element local averaging, the crossover occurred at $p_f=0.5$ whereas by the RFEM it occurred at $p_f\approx 0.38$. The RFEM solutions show that the single random variable approach becomes unconservative over a wider range of V_C values than would be indicated by finite-element local averaging alone.

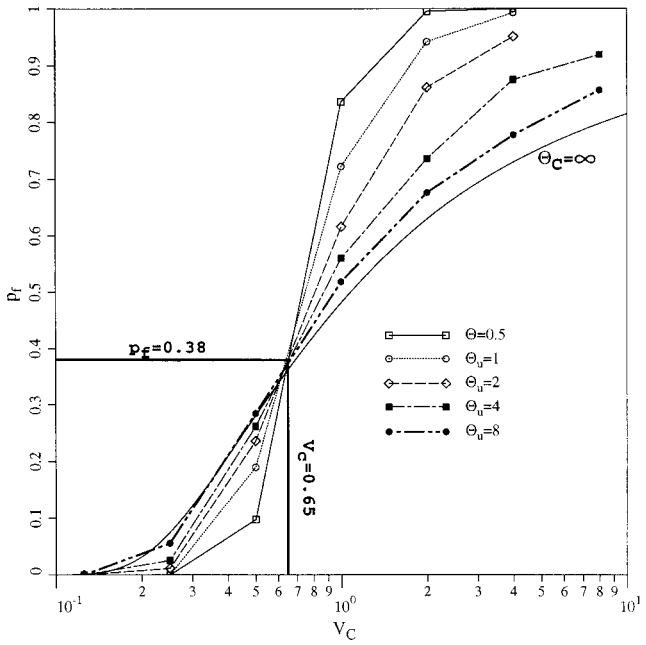

Fig. 17. Probability of failure versus coefficient of variation from random finite-element method; the mean is fixed at $\mu_C=0.25$

Fig. 18 gives a direct comparison between Figs. 13 and 16: it indicates clearly that, for higher values of V_C, RFEM always gives a higher probability of failure than using finite-element local averaging alone. This is caused by the weaker elements in the distribution that dominate the strength of the slope and the failure mechanism that seeks out the weakest path through the soil.

At lower values of V_C, the locally averaged results tend to overestimate the probability of failure and give conservative results compared to RFEM. In this case the stronger elements of the slope dominate the solution and the higher median combined with bunching up of the locally averaged solution at low values of Θ_C means that potential failure mechanisms cannot readily find a weak path through the soil.

In all cases, as Θ_C increases, the RFEM and the locally averaged solutions converge on the single random variable solution that corresponds to $\Theta_C=\infty$ with no local averaging. The $p_f=0.28$ value, corresponding to $V_C=0.5$, discussed earlier in the paper is also indicated in Fig. 18.

All of the above results and discussion in ''Results of Random Finite-Element Method Analyses'' so far were applied to the test slope in Fig. 1 with the mean strength fixed at $\mu_C=0.25$, corresponding to a factor of safety (based on the mean) of 1.47. In the next set of results μ_C is varied while V_C is held constant at 0.5. Fig. 19 shows the relationship between FS (based on the mean) and p_f assuming finite-element local averaging only, and Fig. 20 shows the same relationship computed using RFEM.

Fig. 19, based on finite-element local averaging only, shows the full range of behavior for $0\leqslant\Theta_C<\infty$. Fig. 19 shows that Θ_C

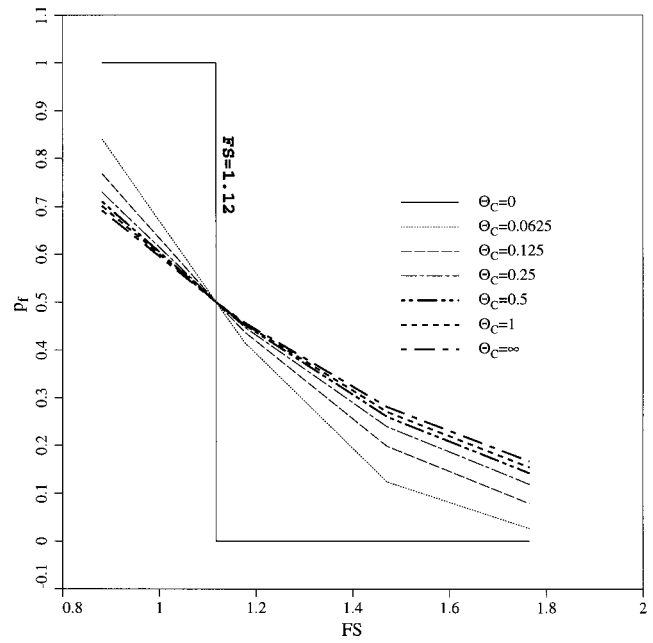

Fig. 19. Probability of failure versus factor of safety (based on the mean) using finite-element local averaging only for the test slope; the coefficient of variation is fixed at $V_C=0.5$

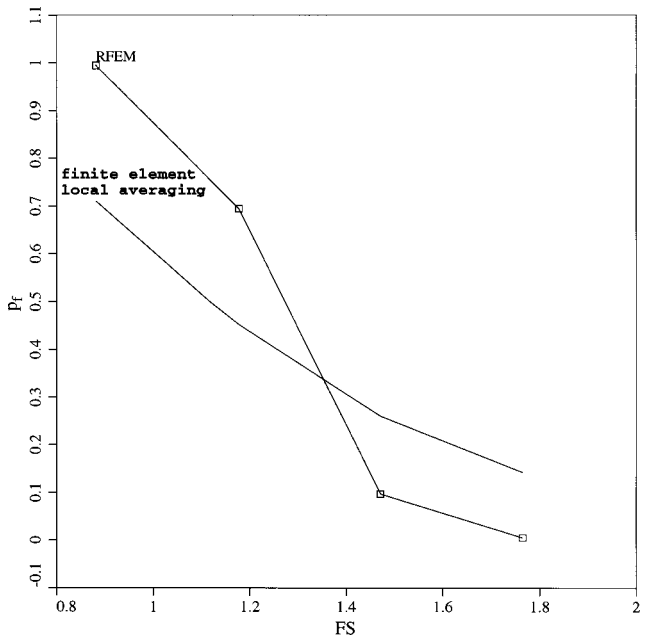

Fig. 21. Probability of failure versus factor of safety (based on the mean) using finite-element local averaging alone and random finite-element method for the test slope; $V_C=0.5$ and $\Theta_C=0.5$

only starts to have a significant influence on the FS versus p_f relationship when the correlation length becomes significantly smaller than the slope height ($\Theta_C \ll 1$). The step function in which p_f jumps from zero to unity occurs when $\Theta_C=0$, and it corresponds to a local average with zero variance. In this limiting case, the local average of the soil is deterministic and yields constant strength everywhere in the slope. With $V_C=0.5$, the critical value of mean shear strength that would give $\mu_{C_A}=\text{median}_C=0.17$ is easily shown by Eq. (22) to be $\mu_C=0.19$, which corresponds to a FS=1.12. For higher values of Θ_C, the relationship between FS and p_f is quite "bunched up," and generally insensitive to Θ_C. For example, there is little difference between the curves corresponding to $\Theta_C=\infty$ and 0.5. It should also be observed in Fig. 19 that, for FS>1.12, failure to account for local averaging by assuming $\Theta_C=\infty$ is conservative, in that the predicted p_f is higher than it should be. When FS<1.12, however, failure to account for local averaging is unconservative.

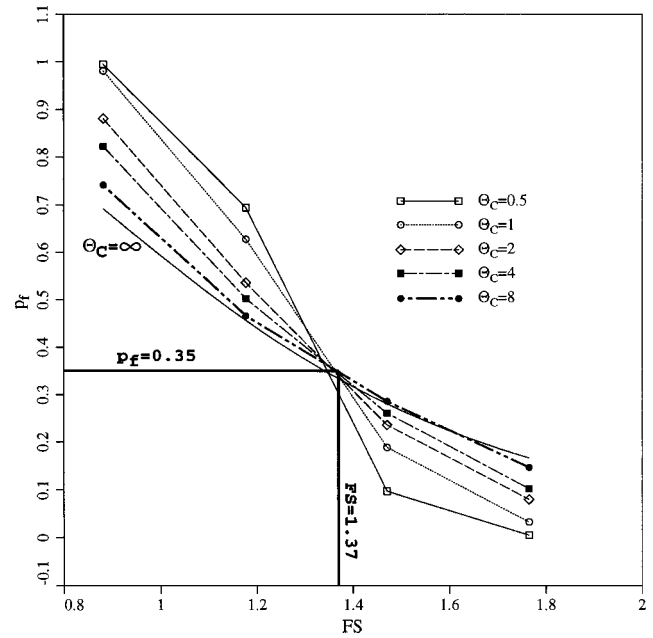

Fig. 20. Probability of failure versus factor of safety (based on the mean) using random finite-element method for the test slope; the coefficient of variation is fixed at $V_C=0.5$

Fig. 20 gives the same relationships as those computed using RFEM. By comparison with Fig. 19, the RFEM results are more spread out, implying that the probability of failure is more sensitive to spatial correlation length Θ_C. Of greater significance is that the crossover point has again shifted by RFEM as it seeks out the weakest path through the slope. In Fig. 20, the crossover occurs at FS≈1.37, which is significantly higher and of greater practical significance than the crossover point of FS≈1.12 by finite-element local averaging alone. The theoretical line corresponding to $\Theta_C=\infty$ is also shown in this plot. From a practical viewpoint, the RFEM analysis indicates that failure to properly account for local averaging is unconservative over a wider range of factors of safety than would be the case by finite-element local averaging alone. To further highlight this difference, the results in Figs. 19 and 20 that correspond to $\Theta_C=0.5$ (the spatial correlation length equal to half the embankment height) are replotted in Fig. 21.

Concluding Remarks

In this paper we have investigated the probability of failure of a cohesive slope using both simple and more advanced probabilistic analysis tools. The simple approach treated the strength of the entire slope as a single random variable, and ignored spatial correlation and local averaging. In the simple studies, the probability of failure was estimated as the probability that the shear strength would fall below a critical value based on a log–normal probabil-

ity density function. These results led to a discussion on the appropriate choice of design shear strength value suitable for deterministic analysis. Two factorization methods were proposed that were able to bring the probability of failure and the factor of safety more into line with practical experience.

The second half of the paper implemented the random finite element method on the same test problem. The nonlinear elastoplastic analyses with Monte Carlo simulation were able to take into full account spatial correlation and local averaging, and observe their impact on the probability of failure using a parametric approach. The elastoplastic finite-element slope stability method makes no a priori assumptions about the shape or location of the critical failure mechanism, and therefore offers very significant benefits over traditional limit equilibrium methods in the analysis of highly variable soils. In the elastoplastic RFEM, the failure mechanism is free to seek out the weakest path through the soil and it has been shown that this phenomenon can lead to higher probabilities of failure than could be explained by local averaging alone.

In summary, simplified probabilistic analysis, in which spatial variability is ignored by assuming perfect correlation, can lead to unconservative estimates of the probability of failure. This effect is most pronounced at relatively low factors of safety (Fig. 20) or when the coefficient of variation of the soil strength is relatively high (Fig. 18).

Acknowledgment

The results shown in this paper are part of a much broader study into the influence of soil heterogeneity on stability problems in geotechnical engineering. The writers wish to acknowledge the support of NSF Grant No. CMS-9877189.

Notation

The following symbols were used in this paper:

C = dimensionless shear strength;
C_{des} = design value of C;
c_u = undrained shear strength;
D = foundation depth ratio;
f_1 = linear strength reduction factor;
f_2 = strength reduction factor based on standard deviation;
H = height of slope;
p_f = probability of failure;
V_C = coefficient of variation of C;
x = Cartesian x coordinate;
y = Cartesian y coordinate;
α = dimensionless element size parameter;
β = slope angle;
γ = variance reduction factor;
γ_{sat} = saturated unit weight;
Θ_C = dimensionless spatial correlation length of $\ln C$;
θ_C = spatial correlation length of C;
$\theta_{\ln C}$ = spatial correlation length of $\ln C$;
μ_C = mean of C;
μ_{C_A} = locally averaged mean of C over a square finite element;
$\mu_{\ln C}$ = mean of $\ln C$;
$\mu_{\ln C_A}$ = locally averaged mean of $\ln C$ over a square finite element;
ρ = correlation coefficient;
σ_C = standard deviation of C;
σ_{C_A} = locally averaged standard deviation of C over a square finite element;
$\sigma_{\ln C}$ = standard deviation of $\ln C$
$\sigma_{\ln C_A}$ = locally averaged standard deviation of $\ln C$ over a square finite element;
τ = absolute distance between two points;
τ_x = x-component of distance between two points;
τ_y = y-component of distance between two points; and
ϕ_u = undrained friction angle.

References

Alonso, E. E. (1976). ''Risk analysis of slopes and its application to slopes in Canadian sensitive clays.'' *Geotechnique*, 26, 453–472.

Bishop, A. W. (1955). ''The use of the slip circle in the stability analysis of slopes.'' *Geotechnique*, 5(1), 7–17.

Chowdhury, R. N., and Tang, W. H. (1987). ''Comparison of risk models for slopes.'' *Proc., 5th Int. Conf. on Applications of Statistics and Probability in Soil and Structural Engineering*, 2, 863–869.

Christian, J. T. (1996). ''Reliability methods for stability of existing slopes.'' *Uncertainty in the geologic environment: From theory to practice, Geotechnical Special Publication No. 58*, C. D. Shackelford et al., eds., ASCE, New York, 409–418.

Christian, J. T., Ladd, C. C., and Baecher, G. B. (1994). ''Reliability applied to slope stability analysis.'' *J. Geotech. Eng.*, 120(12), 2180–2207.

D'Andrea, R. A., and Sangrey, D. A. (1982). ''Safety factors for probabilistic slope design.'' *J. Geotech. Eng. Div., Am. Soc. Civ. Eng.*, 108(9), 1108–1118.

Duncan, J. M. (2000). ''Factors of safety and reliability in geotechnical engineering.'' *J. Geotech. Geoenviron. Eng.*, 126(4), 307–316.

El-Ramly, H., Morgenstern, N. R., and Cruden, D. M. (2002). ''Probabilistic slope stability analysis for practice.'' *Can. Geotech. J.*, 39, 665–683.

Fenton, G. A., and Griffiths, D. V. (1993). ''Statistics of flow through a simple bounded stochastic medium.'' *Water Resour. Res.*, 29(6), 1825–1830.

Griffiths, D. V., and Fenton, G. A. (2000). ''Influence of soil strength spatial variability on the stability of an undrained clay slope by finite elements.'' *Slope Stability 2000, Proc., GeoDenver 2000*, 184–193, ASCE, New York.

Griffiths, D. V., and Fenton, G. A. (2001). ''Bearing capacity of spatially random soil: The undrained clay Prandtl problem revisited.'' *Geotechnique*, 51(4), 351–359.

Griffiths, D. V., and Lane, P. A. (1999). ''Slope stability analysis by finite elements.'' *Geotechnique*, 49(3), 387–403.

Fenton, G. A., and Vanmarcke, E. H. (1990). ''Simulation of random fields via local average subdivision.'' *J. Eng. Mech.*, 116(8), 1733–1749.

Hassan, A. M., and Wolff, T. F. (2000). ''Effect of deterministic and probabilistic models on slope reliability index.'' *Slope Stability 2000, Geotechnical Special Publication No. 101*, D. V. Griffiths et al., eds., ASCE, New York, 194–208.

Kulhawy, F. H., Roth, M. J. S., and Grigoriu, M. D. (1991). ''Some statistical evaluations of geotechnical properties.'' *Proc., ICASP6, 6th Int. Conf. on Applied Statistics Probability in Civil Engineering*.

Lacasse, S. (1994). ''Reliability and probabilistic methods.'' *Proc., 13th Int. Conf. on Soil Mechanics Foundation Engineering*, 225–227.

Lacasse, S., and Nadim, F. (1996). ''Uncertainties in characterising soil properties.'' *Geotechnical Special Publication No. 58, Proc., Uncertainity '96*, C. D. Shackelford et al., eds., ASCE, New York, 49–75.

Lee, I. K., White, W., and Ingles, O. G. (1983). *Geotechnical engineering*, Pitman, London.

Li, K. S., and Lumb, P. (1987). ''Probabilistic design of slopes.'' *Can. Geotech. J.*, 24, 520–531.

Matsuo, M., and Kuroda, K. (1974). ''Probabilistic approach to the design of embankments.'' *Soils Found.*, 14(1), 1–17.

Mostyn, G. R., and Li, K. S. (1993). ''Probabilistic slope stability—State of play.'' *Proc., Conf. on Probabilistic Methods in Geotechnical Engineering*, K. S. Li and S.-C. R. Lo, eds., 89–110, Balkema, Rotterdam, The Netherlands.

Mostyn, G. R., and Soo, S. (1992). ''The effect of autocorrelation on the probability of failure of slopes.'' *6th Australia, New Zealand Conf. on Geomechanics: Geotechnical Risk*, 542–546.

Paice, G. M. (1997). ''Finite element analysis of stochastic soils.'' PhD thesis, Univ. of Manchester, Manchester, U.K.

Smith, I. M., and Griffiths, D. V. (1998). *Programming the finite element method*, 3rd Ed., Wiley, Chichester, U.K.

Tang, W. H., Yucemen, M. S., and Ang, A. H. S. (1976). ''Probability-based short-term design of slopes.'' *Can. Geotech. J.*, 13, 201–215.

Taylor, D. W. (1937). ''Stability of earth slopes.'' *J. Boston Soc. Civ. Eng.*, 24, 197–246.

Vanmarcke, E. H. (1977). ''Reliability of earth slopes.'' *J. Geotech. Eng. Div., Am. Soc. Civ. Eng.*, 103(11), 1247–1265.

Vanmarcke, E. H. (1984). *Random fields: Analysis and synthesis*, MIT Press, Cambridge, Mass.

Whitman, R. V. (2000). ''Organizing and evaluating uncertainty in geotechnical engineering.'' *J. Geotech. Geoenviron. Eng.*, 126(7), 583–593.

Wolff, T. F. (1996). ''Probabilistic slope stability in theory and practice.'' *Uncertainty in the geologic environment: From theory to practice, Geotechnical Special Publication No. 58*, C. D. Shackelford et al., eds., ASCE, New York, 419–433.